

Benjamin O. EZURIKE ¹, Stephen A. AJAH ¹,
Uchenna NWOKENKWO ¹, Chukwunenye A. OKORONKWO ¹

Modeling and analysis of energy and exergy performance of a PCM-augmented concrete-based Trombe wall systems

Received 27 September 2021, Revised 28 November 2021, Accepted 3 January 2022, Published online 31 March 2022

Keywords: Trombe wall, boundary condition, thermal storage, simulation

The aim of this research was to model the performances of energy and exergy on a Trombe wall system to enable an adequate thermal comfort. The main equations for the heat transfer mechanisms were developed from energy balances on subcomponents of the Trombe wall with the specification of the applicable initial and boundary conditions. During the incorporation of the PCM on the Trombe wall, the micro-encapsulation approach was adopted for better energy conservation and elimination of leakage for several cycling of the PCM. The charging and discharging of the PCM were equally accommodated and incorporated in the simulation program. The results of the study show that an enhanced energy storage could be achieved from solar radiation using PCM-augmented system to achieve thermal comfort in building envelope. In addition, the results correspond with those obtained from comparative studies of concrete-based and fired-brick augmented PCM Trombe wall systems, even though a higher insolation was used in the previous study.

1. Introduction

Every building envelope is saddled with the aim of protecting its occupants from extreme harsh weather conditions as well as providing thermal comfort. Hence, the utilization of solar energy in achieving thermal comfort has been getting global attention. It can be done through the application of translucent thermal insulation used as the coating features in a passive solar structure, to ensure an

✉ Benjamin O. Ezurike, e-mail: ben4oke2000@yahoo.com

¹Department of Mechanical/ Mechatronics Engineering, Alex Ekwueme Federal University Ndufu-Alike, Nigeria. ORCIDs: B.O.E.: 0000-0002-1311-5355; S.A.A.: 0000-0002-2034-3049; U.N.: 0000-0001-7044-1846; C.A.O.: 0000-0002-5098-9764



© 2022. The Author(s). This is an open-access article distributed under the terms of the Creative Commons Attribution-NonCommercial-NoDerivatives License (CC BY-NC-ND 4.0, <https://creativecommons.org/licenses/by-nc-nd/4.0/>), which permits use, distribution, and reproduction in any medium, provided that the Article is properly cited, the use is non-commercial, and no modifications or adaptations are made.

adequate thermal wellbeing in a built environment [1]. Achieving of thermal comfort in a building (which is a function of the preferred temperature of about 28°C for tropical regions like Nigeria) was previously done through the use of air conditioners. However, this is usually associated with a greater energy consumption. As a result, possible ways of reducing such a high energy used for heating and cooling in continuous international house envelopment expansion, that amounts to the fraction of 0.4 of the gross used energy, is an important approach to be adopted for greenhouse gas emissions reduction [2]. Trombe wall is one of the most predominant passive structures which utilize the sun radiation energy for warming, cooling, ventilating and ensuring adequate relaxation in buildings [3]. Fig. 1 shows a typical Trombe wall system which is made of a high thermal mass black painted wall usually facing eastward. The solar fluxes radiating through the glazing are usually absorbed by the black painted surfaces which are contained within the Trombe wall, and the energy can be extracted when needed in the room space through the use of the incorporated vents [4]. The vents and the insulation components of the Trombe wall are incorporated in such a manner as to control the release of the thermal energy. With the use of Trombe wall technology, energy consumption in a house can be reduced even to 30% [3].

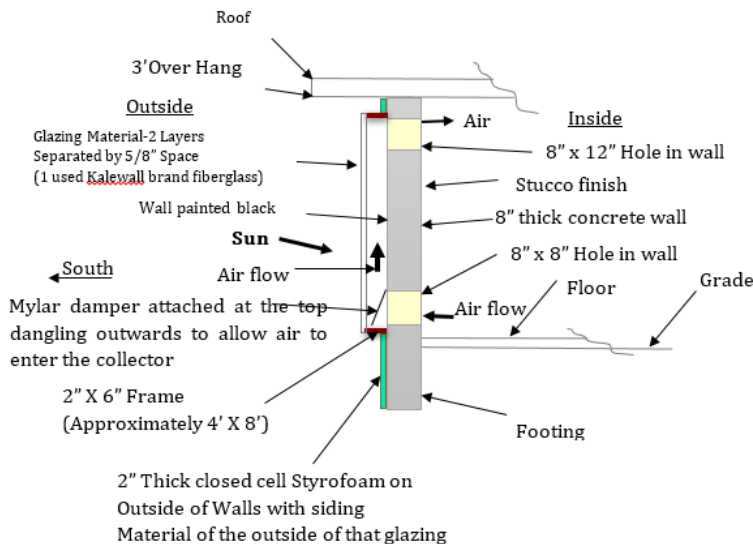


Fig. 1. Conventional Trombe wall with airgap and vents [4]

The wall may be constructed with a concrete-based material, solid fired red bricks or even a phase change material (PCM), but it is usually detached from the free ambient environment by the use of a single or double glazing with a light air gap that separates them.

1.1. Phase Change Materials

The loading of thermal energy into a house envelope can be done with the use of several media like paraffins, stones, water, concrete as well as the PCMs. Unlike the PCMs, other media require a high volume for storing a significant amount of energy to be used [2]. Energy accumulation and release processes in such systems do not occur at an almost constant temperature, like in the case of PCMs, which results in their remarkably poorer performance and low efficiency [5]. With the application of the PCMs for safe-keeping of energy, higher energy storage densities can be achieved, while the heat is stored and released isothermally, unlike the cases of water and concrete.

1.2. Applications of Trombe walls

Numerous researches have been carried out in the past decades by solar energy experts on the Trombe wall as an efficient passive solar structural method. Sankaranarayanan et al. [6] used a Trombe wall in a study on effectiveness and continuous improvement within the businesses in energy and chemical industries. Kuznik and Virgone [7] experimentally assesses PCMs performance for building purposes. Feldman et al. [8] investigated the application of the Trombe wall with the application of solidity of biological mixtures including fatty acids for dormant temperature keeping. The utilization of this stored heat above a desired inside temperature variation in houses could lead to an upsurge in the thermal storage capacity ranging from 10 to 30% [9].

1.3. Trombe walls performance assessment

The performance of such a system virtually depends on thermal conductivity of the wall construction materials as well as the airflow characteristics in the air gap of the Trombe wall [6]. Okonkwo and Akubuo [9] carried out an experimental study for Trombe wall thermal assessment in poultry brooding, which showed that brooding temperature range between 28°C and 35°C could be maintained, and their results indicate the ability of the Trombe wall system to moderate the temperature fluctuations within a poultry house. However, the authors did not carry out a mathematical analysis with regard to energy or exergy flow in the system. Cao et al. [10] in their studies found that, with PCM incorporation in a building, about 37% energy saving was recorded. In a numerical study done by Abbassi and Dehmani [11], a classical unvented Trombe wall system was associated with a fresh one comprising internal thermal fins. Huang et al. [12] carried out numerical evaluation for Trombe wall energy conservation, and they found that the Trombe wall system built of PCM-augmented materials (composite material based Trombe wall) had a higher energy efficiency than the conventional Trombe wall in cold and muddy climate.

Incorporation of a PCM in the concrete-based Trombe wall is very important for improving its energy performance and for controlling the cost associated with environment energy savings. Temporal temperature variation of the building envelope components including the vents, airgap and glazing, which wasn't verified by other researchers, has been evaluated in this study. Adjustable vents were introduced in Trombe wall systems to accommodate their applications not only for heating but also for cooling a building in tropical regions. Mathematical analysis are novelties in Trombe wall research have been included.

2. Methodology

Mathematical model of thermal energy flows in the system is presented for determining temperature distribution in the system. Next, equations are presented for computing the exergy flows in the system based on the temperature distributions in the system. Finally, energy and exergy efficiency expressions are presented for evaluating the performance of the system as shown in Fig. 2.

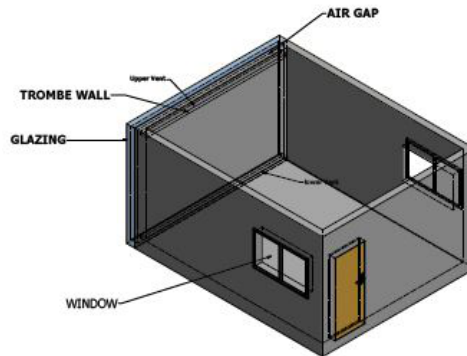


Fig. 2. Trombe wall diagram with the associated convectational vents

$$\rho C_p \frac{\partial}{\partial t} \int_V T dV = - \int_A \dot{q} dA + \int_V B dV. \quad (1)$$

In the above equation, ρ is the density of the wall material (Kg/m^3), C_p is the specific heat capacity (J/(kg K)), T is Temperature (K), dV is the change in volume (m^3), q is the vectoral heat flux (W/m^2), dA is the vectoral node surface area (m^2), B is the internal heat generation per unit volume (J/m^3).

Equation (1) is the transient control volume energy equation for a thermal system. The left-hand side (LHS) of Equation (1) is the enthalpy accumulation rate within the control volume, the first term of the right-hand side (RHS) of the equation is the frequency at which the heat is transferred across the surfaces, while the last term of the RHS is the rate of internal heat generation in the system. When

there is no heat generation, $B = 0$. After a simplification, Equation (1) becomes similar to that evaluated by Ajah et al. [13] in their previous study.

$$\frac{\partial h}{\partial t} = \frac{\lambda_x^-}{\Delta x} \left(\frac{\partial T}{\partial x} \right)^- + \frac{\lambda_x^+}{\Delta x} \left(\frac{\partial T}{\partial x} \right)^+ - \frac{\lambda_y^-}{\Delta y} \left(\frac{\partial T}{\partial y} \right)^- + \frac{\lambda_y^+}{\Delta y} \left(\frac{\partial T}{\partial y} \right)^+. \quad (2)$$

Incorporation of the PCM as an enhanced enthalpy storage medium results in a change in the system thermo-physical behavior compared to the case of pure concrete due to the phase change occurring throughout the melting and solidification stages. This sum of the enthalpy is given as h_T and represented thus:

$$h_T = \rho C_p T + \rho L_f f, \quad (3)$$

where $h_f = \rho L_f f$, which is equal to specific heat accumulated within the control volume (CV), L_f denotes latent heat of fusion, f is liquid fraction of the PCM when melting

$$\frac{\partial h_T}{\partial t} = \frac{\alpha_x^-}{\Delta x} \left(\frac{\partial h}{\partial x} \right)^- + \frac{\alpha_x^+}{\Delta x} \left(\frac{\partial h}{\partial x} \right)^+ - \frac{\alpha_y^-}{\Delta y} \left(\frac{\partial h}{\partial y} \right)^- + \frac{\alpha_y^+}{\Delta y} \left(\frac{\partial h}{\partial y} \right)^+, \quad (4)$$

where α is the thermal diffusivity of the medium given by: $\frac{\lambda}{\rho C_p}$; λ is the thermal conductivity of the medium (W/(m K)), ρ is the density of the medium (kg/m³) and C_p is the specific heat capacity (J/(kg K)).

At the beginning, the enthalpy h is even all over and within the partition, that is

$$h(x, y, 0) = h_{ini}, \quad (5)$$

$h_{ini} = m C_p T_{ini}$ represents the first thermal energy in the partition with the first undeviating temperature of T_{ini} .

2.1. Energy equation discretization of the Trombe wall

The system is discretized in such a way that its thickness L is distributed amongst n sheets of wideness Δx along the direction of x , while its tallness H is divided into m films of tallness Δy in the y route. Hence, $\Delta x = \frac{L}{n}$, $\Delta y = \frac{H}{m}$. The temporal discretization was in Δt time steps.

$$\begin{aligned} \frac{h_{T(i,j)}^{k+1} - h_{T(i,j)}^k}{\Delta t} &= \frac{\alpha_x^-}{\Delta x} \left(\frac{h_{i,j}^k - h_{i-1,j}^k}{\Delta x} \right)^- + \frac{\alpha_x^+}{\Delta x} \left(\frac{h_{i+1,j}^k - h_{i,j}^k}{\Delta x} \right)^+ - \frac{\alpha_y^-}{\Delta y} \left(\frac{h_{i,j}^k - h_{i,j-1}^k}{\Delta y} \right)^- \\ &+ \frac{\alpha_y^+}{\Delta y} \left(\frac{h_{i,j+1}^k - h_{i,j}^k}{\Delta y} \right)^+. \end{aligned} \quad (6)$$

Equation (6) can further be simplified as

$$h_{T(i,j)}^{k+1} = h_{T(i,j)}^k - h_{i,j}^k \text{Fo}_{i,j} + \text{Fo}_{i,j}^{x+} h_{i+1,j}^k + \text{Fo}_{i,j}^{x-} h_{i-1,j}^k + \text{Fo}_{i,j}^{y+} h_{i,j+1}^k + \text{Fo}_{i,j}^{y-} h_{i,j-1}^k. \quad (7)$$

The energy balance for the borderline nodes can be disjointedly considered.

For the glazing side wall

$$h_{T(i,j)}^{k+1} = h_{T(i,j)}^k - h_{i,j}^k (\text{Fo}_{i,j}^{x+} + \text{Fo}_{i,j}^{y-} + \text{Fo}_{i,j}^{y+}) + \frac{\Delta t \tau_g \alpha_w I_{\text{sun}}}{\Delta x} + \text{Fo}_{i,j}^{y-} h_{i,j-1}^k + \text{Fo}_{i,j}^{y+} h_{i,j+1}^k + \frac{\Delta t}{\Delta x} + \text{Fo}_{i,j}^{x+} h_{2j}^k. \quad (8)$$

With respect to the room side

$$h_{T(n,j)}^{k+1} = h_{T(n,j)}^k - h_{n,j}^k (\text{Fo}_{n,j}^{x-} + \text{Fo}_{n,j}^{y-} + \text{Fo}_{n,j}^{y+}) + \text{Fo}_{n,j}^{x-} h_{n-1,j}^k + \frac{\Delta t}{\Delta x} [h_{\text{conv},w-r} (T_{n,j}^k - T_R^k)] + \text{Fo}_{n,j}^{y-} h_{n,j-1}^k + \text{Fo}_{n,j}^{y+} h_{n,j+1}^k. \quad (9)$$

For upper vent side

$$h_{T(i,m)}^{k+1} = h_{T(i,m)}^k + \text{Fo}_{i,m}^{y-} h_{i,m-1}^k - h_{i,m}^k \text{Fo}_{i,m}^x - h_{i,m}^k (\text{Fo}_{i,m}^{x-} + \text{Fo}_{i,m}^{y-}) + \text{Fo}_{i,m}^{x+} h_{i+1,m}^k + \frac{\Delta t}{\Delta y} [h_{\text{conv},Uv} (T_{i,m}^k - T_{\text{vent,out}}^k)] + \text{Fo}_{i,m}^{x-} h_{i-1,j}^k. \quad (10)$$

For the lower vent side

$$h_{T(i,1)}^{k+1} = h_{T(i,1)}^k - h_{i,1}^k (\text{Fo}_{i,1}^{y+} + \text{Fo}_{i,1}^{x-} + \text{Fo}_{i,1}^{x+}) + \text{Fo}_{i,1}^{x-} h_{i-1,1}^k + \text{Fo}_{i,1}^{x+} h_{i+1,1}^k + \text{Fo}_{i,1}^{y+} h_{i,2}^k + \frac{\Delta t}{\Delta y} [h_{\text{conv},Lv} (T_{i,1}^k - T_{\text{vent,in}}^k)]. \quad (11)$$

The total stored enthalpy h_T^{k+1} within the wall during the period $k+1$ is expressed as: $n-1, m-1$.

$$h_{KT+1} = h_{KT+1(1,j)} + h_{KT+1(i,1)} + h_{KT+1(i,j)} + h_{KT+1(n,j)} + h_{KT+1(i,m)}. \quad (12)$$

The stored energy within the wall can be expressed as:

$$\Delta E^k = \sum_{i,j} m_{ij} c_{p,ij} [(T_{ij}^k - T_{ij}^{\text{ini}})], \quad (13)$$

$i = 2, j = 2$.

The exergy $\Delta \Xi$ contained in the Trombe wall is given by:

$$\Delta \Xi = \Delta E - T_a \Delta s. \quad (14)$$

In regard to temperatures in the wall,

$$\Xi = \sum_{i,j} m_{ij} c_{p,ij} (T_{ij} - T_{ini}) - \sum_{ij} m_{ij} c_p T_a \ln \left(\frac{T_{ij}}{T_{ini}} \right). \quad (15)$$

Equation (15) gives the expression for the exergy storage in the wall as a function of the wall temperature. In this equation, m_{ij} is the mass of each cell (kg), $c_{p,ij}$ denotes the specific heat capacity (J/(kg K)), T_{ini} represents initial temperature of the wall (K), T_{ij} is the wall temperature (K) and T_a is the ambient heat (K).

2.2. Efficiencies

The system is discretized in such a way that its thickness L is distributed amongst n sheets of wideness Δx along the direction of x , while its tallness H is divided into m films of tallness Δy in the y route. Hence, the energy efficiency of the system can be calculated as follows;

$$\eta_I^k = \frac{\Delta E^k \cdot 100}{\sum_k \tau_g \alpha_w A_g I_{\text{sun}} \Delta t}, \quad (16)$$

where A_g denotes heat transfer surface area of the glazing, I_{sun} is solar radiation intensity.

Equation (16) was used to compute the energy efficiency of the system, and has been solved by the Scilab computer program.

2.3. Second law efficiency

The arrangement of this η_{II} can be found using,

$$\eta_{II} = \frac{\Delta \Xi}{\Xi_{\text{in}}}, \quad (17)$$

where,

$$\Xi_{\text{in}} = \Xi_{\text{sun}} = X \psi \tau_g \alpha_w A_g I_{\text{sun}} \Delta t, \quad (18)$$

where ψ is expressed as [14]

$$\psi = 1 - \frac{4}{3} \left(\frac{T_o}{T_s} \right) + \frac{1}{3} \left(\frac{T_o}{T_s} \right)^4. \quad (19)$$

Equations (17)–(19) were used for the computation of the exergy and were solved with the Scilab computer program. This gives the efficiency which a real system can deliver while considering the irreversibility of a functional system.

3. Results

3.1. Phase Change Materials

The modelled equations were solved with Scilab program for the energy stored and temperature profiles evaluation, using the time step of $\Delta t = 10$ seconds. The Trombe wall construction parameters were also used in the Scilab program to obtain the solution to the respective equations. The Emerest2325 was the PCM chosen for this research based on its thermophysical characteristics (thermal conductivity of 0.726 W/(mK) , density of 1601 kg/m^3 , specific heat capacity of 836 J/(kg K) and latent heat of fusion 0.1384 MJ/kg). The Emerest2325 does not affect the thermophysical properties of the cement when mixed together [15]. The daily ambient temperature and insolation variation were used as the main independent parameters for the system simulation, respectively, as shown in Fig. 3.

Table 1. Different wall simulation parameters with their thermophysical properties

Materials	λ (W/mK)	ρ (kg/m ³)	C_p (J/kgK)	L_f (MJ/kg)	T_m (°C)
Concrete	0.733	2314	800		
PCM	0.726	1601	836	0.1384	28–30

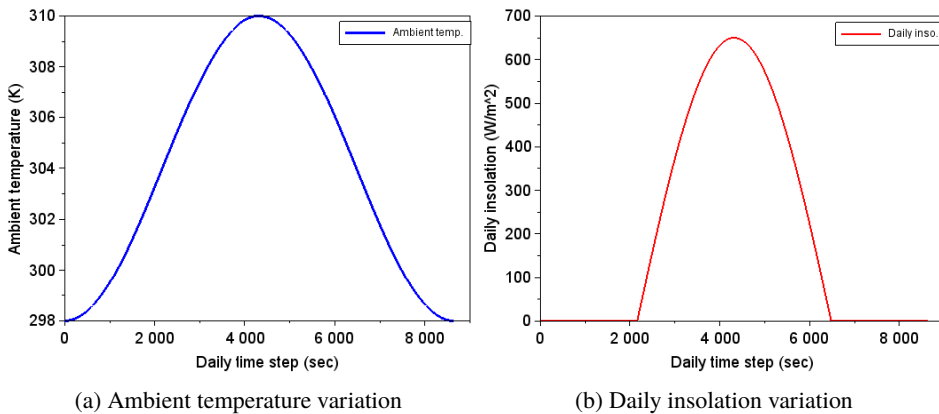


Fig. 3. Daily ambient temperature and insolation

In Fig. 3a, the ambient temperature varies from 25°C (298 K) during the night and morning period to 37°C (310 K) during the midday period when the insolation is usually at the peak. The gradual increase in the ambient temperature from the morning to midday was also maintained during the decreasing period, which was the solar radiation intensity reduction period. Meanwhile, a similar trend was also maintained for the case of daily insolation variation, as shown in Fig. 3b. The insolation gradually increases from 0 W/m^2 during the night and morning period to 665 W/m^2 during the midday period.

3.2. Energy and exergy stored fluctuation in the Trombe partition

The equations of reserved energy of the wall were modeled and solved with a carefully written Scilab software package to determine the stored net system energy of Equation (12) and the deviation at regular hours was graphed for a week, as shown in Fig. 4.

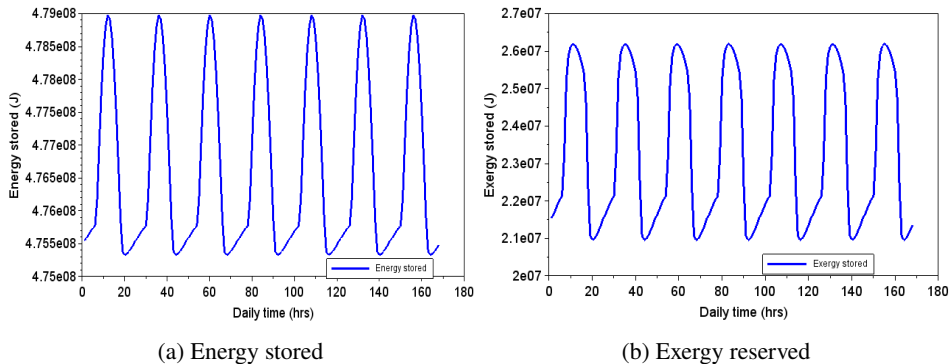


Fig. 4. Wall energy and exergy accumulated

During the morning, the initial energy stored in the system was recorded to be 475.3 MJ, and it gradually increased when the sun rose. A continuous increment of the stored energy was also observed as the daily insolation increased attaining the maximum point of 479.5 MJ within the mid-day with an energy gain of approximately 4.2 MJ. The energy storage reduces with the solar radiation intensity around the evening and regains its initial value in the night with a repeated occurrence for the seven simulated days. Equation (15) was used for the computation of the stored exergy within the Trombe wall. The total accumulated exergy in the system was plotted as shown in Fig. 4b. The observed stored exergy profile was similar to that of the energy stored with initial and final values of 21.4 MJ and 26.8 MJ during night/early morning and midday respectively, repeatedly for the seven days.

3.3. Trombe wall energy and exergy efficiencies

The system energy efficiency was computed on daily hourly basis for a week using equation 16 with a Scilab program. It was observed that it had a similar profile as the stored enthalpy graph. From Fig. 5a, one observes a rise in efficiency of the system as daily insolation keeps increasing and it gradually moves from 42.74% during the night period to 43.07% at midday. Similarly, the system exergy efficiency was computed with Equation (17) using the Scilab program and was plotted against time, as shown in Fig. 5b. This second law efficiency has the same

trend as that obtained in first law efficiency case with the values changing from 2.05% in the night to 2.56% around midday, repeatedly for a week.

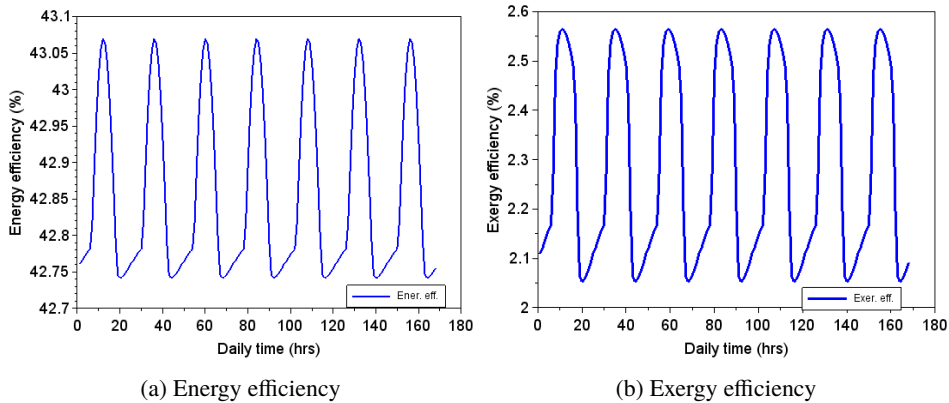


Fig. 5. Energy and exergy efficiency of the system

The study has shown that a greater solar radiation energy storage can be realized by using the PCM-augmented system to achieve thermal comfort in a building envelope. The results correspond with those obtained by [13] in a comparative study on concrete-based and fired-brick augmented PCM Trombe wall system though with higher insolation.

For the validation of this model, the wall temperature results were compared with the ones obtained by [11] in their experiment using a test room of dimensions 0.8 m by 0.9 m by 0.9 m. It was observed that the peak wall temperature experimental result was 59°C (332 K) compared with the present model peak temperature of 317 K (44°C) with 40.2% efficiency, even though the wall dimensions were different. This study is limited to building geometry of rectangular shape, hence the use of Cartesian coordinates in the analysis. It is also limited to a two-dimensional (2-D) problem, hence the 2-D analysis was adopted.

The original development of this research is the use of finite volume differential analysis with fully explicit discretization approach for the determination of the flow of energy and exergy in the PCM-augmented method to achieve thermal comfort. One difficulty that could be encountered consists in obtaining the timely and smooth convergence of the solution if a greater time step is used for the simulation, hence very short-time step of 10 seconds is ideal.

The drawback of this study could be the errors resulting from the use of the model to simulate the real-life scenario due to the variability and fluctuations of solar radiation on daily basis, which is different from the steady and invariable case adopted in this study. These errors can be eliminated by building a practical system, generating some data of temperature and other relevant parameters to produce real and accurate models.

3.4. Model validation

The results were compared with those obtained by other experimental researchers. The concrete outer wall temperature was compared with the result obtained by Abbassi and Dehmani [11] in their experimental study at the laboratory of thermal process in Borj Cedria in Tunisia using a test room of the size of 0.9 m by 0.9 m by 0.8 m. Fig. 6 shows the comparison of the two results. A similar condition, of no fins attached to the wall, was used for the experimental case and was also used for the numerical model. It can be seen that the experimental value from that study for the maximum wall temperature is 58°C while the present model gives a maximum temperature of 326 K (53°C). The minimum temperature obtained by the other researchers is 20°C, which is the same as that obtained from the present model. A discrepancy in the maximum temperature between the experimental and model results equals 6.91%. This is possibly due to the effects of some parametric environmental conditions like relative humidity, surrounding air velocity and pressure, and some technical errors that may occur during the experimental studies. Nevertheless, the discrepancy is not too high, and the method can be used for the validation of numerical models.

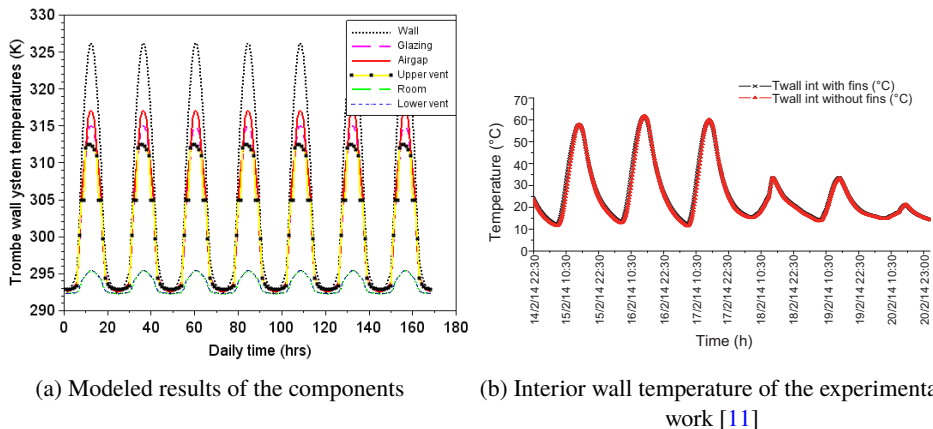


Fig. 6. Research validation with an experimental work

4. Conclusions

Modeling of the transient energy and exergy flows in PCM-augmented concrete Trombe wall systems had been done through finite volume discretization using an explicit method. The maximum stored exergy as well as the energy in the system with the respective efficiencies were found to be 479.5 MJ and 26.8 MJ with 43.02% and 2.56%. This shows that the energy of a real system must be greater than the exergy of the system due the some wasted part of the system energy in the form of exergy destruction, which is in line with the claim of the second law of

thermodynamics. The destroyed exergy is as a result of irreversibility of the system. The results concerning the stored energy and exergy are in line with those obtained by [13] in a comparative study on concrete-based and fired-brick augmented PCM Trombe wall system, even though the other authors' system was provided with a higher insolation.

Acknowledgements

The authors wish to thank the department of Mechanical/Mechatronics Engineering Federal University of Technology, Owerri and the department of Mechanical/Mechatronics Engineering, Alex Ekwueme Federal University Ndufu-Alike for their assistance during this research. We also wish to express our gratitude to management of Alex Ekwueme Federal University Ndufu-Alike for providing an enabling environment during this study.

References

- [1] I. Blasco Lucas, L. Hoesé, and D. Pontoriero. Experimental study of passive systems thermal performance. *Renewable Energy*, 19(1-2):39–45, 2000. doi: [10.1016/S0960-1481\(99\)00013-0](https://doi.org/10.1016/S0960-1481(99)00013-0).
- [2] A. Mastrucci. *Experimental and Numerical Study on Solar Walls for Energy Saving, Thermal Comfort and Sustainability of Residential Buildings*. Ph.D. Thesis, University Politecnica delle Marche, Italy, 2013.
- [3] A. Chel, J.K. Nayak, and G. Kaushik. Energy conservation in honey storage building using Trombe wall. *Energy and Building*, 40(9):1643–1650, 2008. doi: [10.1016/j.enbuild.2008.02.019](https://doi.org/10.1016/j.enbuild.2008.02.019).
- [4] L. Zalewski, A. Joulin, S. Lassue, Y. Dutil, and D. Rousse. Experimental study of small-scale solar wall integrating phase change material. *Solar Energy*, 86(1):208–219, 2012. doi: [10.1016/j.solener.2011.09.026](https://doi.org/10.1016/j.solener.2011.09.026).
- [5] C.M. Lai and C.M. Chiang. How phase change materials affect thermal performance: hollow bricks. *Building Research & Information*, 34(2):118–130, 2011. doi: [10.1080/09613210500493197](https://doi.org/10.1080/09613210500493197).
- [6] K. Sankaranarayanan, H.J. van der Kooi, and J. de Swaan Arons. *Efficiency and Sustainability in the Energy and Chemical Industries. Scientific Principles and Case Studies*. CRC Press, Boca Raton, 2010. doi: [10.1201/EBK1439814703](https://doi.org/10.1201/EBK1439814703).
- [7] F. Kuznik and J. Virgone. Experimental assessment of a phase change material for wall building use. *Applied Energy*, 86(10):2038–2046, 2009. doi: [10.1016/j.apenergy.2009.01.004](https://doi.org/10.1016/j.apenergy.2009.01.004).
- [8] D. Feldman, M.M. Shapiro, D. Banu, and C.J. Fuks. Fatty acids and their mixtures as phase-change materials for thermal energy storage. *Solar Energy Materials*, 18(3-4):201–216, 1989. doi: [10.1016/0165-1633\(89\)90054-3](https://doi.org/10.1016/0165-1633(89)90054-3).
- [9] W.I. Okonkwo and C.O. Akubuo. Trombe wall system for poultry brooding. *International Journal of Poultry Science*, 6(2):125–130, 2007. doi: [10.3923/ijps.2007.125.130](https://doi.org/10.3923/ijps.2007.125.130).
- [10] L. Cao, F. Tang, and G. Fang. Synthesis and characterization of microencapsulated paraffin with titanium dioxide shell as shape-stabilized thermal energy storage materials in buildings. *Energy and Buildings*, 72:31–37, 2014. doi: [10.1016/j.enbuild.2013.12.028](https://doi.org/10.1016/j.enbuild.2013.12.028).
- [11] F. Abbassi and L. Dehmani. Experimental and numerical study on thermal performance of an unvented Trombe wall associated with internal thermal fins. *Energy and Buildings*, 105:119–128, 2015. doi: [10.1016/j.enbuild.2015.07.042](https://doi.org/10.1016/j.enbuild.2015.07.042).

- [12] M.J. Huang, P.C. Eames, and N. J. Hewitt. The application of a validated numerical model to predict the energy conservation potential of using phase change materials in the fabric of a building. *Solar Energy Materials and Solar Cells*, 90(13):1951–1960, 2006. doi: [10.1016/j.solmat.2006.02.002](https://doi.org/10.1016/j.solmat.2006.02.002).
- [13] S.A. Ajah, B.O. Ezurike, and H.O. Njoku. A comparative study of energy and exergy performances of a PCM-augmented cement and fired-brick Trombe wall systems. *International Journal of Ambient Energy*, 1–18, 2020. doi: [10.1080/01430750.2020.1718753](https://doi.org/10.1080/01430750.2020.1718753).
- [14] H.O. Njoku, B.E. Agashi, and S.O. Onyegebu. A numerical study to predict the energy and exergy performances of a salinity gradient solar pond with thermal extraction. *Solar Energy*, 157:744–761, 2017. doi: [10.1016/j.solener.2017.08.079](https://doi.org/10.1016/j.solener.2017.08.079).
- [15] C. Ji, Z. Qin, S. Dubey, F.H. Choo, and F. Duan. Three-dimensional transient numerical study on latent heat thermal storage for waste heat recovery from a low temperature gas flow. *Applied Energy*, 205:1–12, 2017. doi: [10.1016/j.apenergy.2017.07.101](https://doi.org/10.1016/j.apenergy.2017.07.101).